Stand-alone WiFi-based Passive Forward Scatter Radar sensor for vehicles classification

M. Stentella, A. Losito, T. Martelli, F. Colone

DIET Dept., Sapienza University of Rome
Via Eudossiana, 18 – 00184 Rome, Italy
{tatiana.martelli, fabiola.colone}@uniroma1.it

Keywords: Passive Forward Scatter radar, WiFi signals, vehicle classification, target motion estimation.

Abstract

Following the promising results obtained in previous studies, in this paper we address the main limitations of a WiFi-based Passive Forward Scatter Radar in vehicles monitoring applications. Specifically, the possibility to operate in the absence of a reference signal is investigated in order to avoid the need for a dedicated receiving channel and to make the sensor independent of the exploited transmitter of opportunity. Moreover, aiming at the automatic classification of surface vehicles, an effective strategy is considered to estimate the target velocity in order to properly scale the corresponding signatures for direct comparison. The proposed approaches are extensively tested against experimental datasets in order to verify their practical feasibility.
This paper is a companion to another paper submitted to this conference [1]. Specifically, with the proposed approaches we complement and extend the results in [1] by providing an effective solution for a realistic implementation of the conceived sensor.

1 Introduction

In a companion paper submitted to this conference [1], we have shown that a WiFi-based passive radar system can be successfully exploited for surface vehicles automatic classification by adopting a forward scatter radar geometry, i.e. an extreme bistatic configuration where the bistatic angle is close to 180°. In fact, thanks to the "forward scattering" mechanism that is invoked to model the transmitted energy scattered by the target [2],[8], quite stable profiles are observed in the received signals when a given vehicle repeatedly crosses the transmitter (Tx) - receiver (Rx) baseline. These profiles were shown to be characteristic signatures of the specific target so that they could be easily exploited by a proper automatic classification stage [1].
However, the procedure adopted in [1] to extract the vehicles signature from the received signals yields some intrinsic limitations. Basically, being that work mostly focused on the subsequent classification stage, the signature extraction was based on two restrictive assumptions:

(i) the availability of a good copy of the transmitted signal, namely the reference signal, and
(ii) the availability of an accurate estimate of the target cross-baseline velocity component, that is critical to obtain the required resampling of the different signatures for a direct comparison [3].

The first assumption is a legacy from a conventional passive radar operation and potentially allows to preserve the target detection capability of the conceived sensor even outside the forward scatter region in the strictest sense. Obviously, this assumption yields the requirement for a dedicated receiving channel to collect the signal from the (possibly cooperative) transmitter [4].
In this paper, aiming at reducing the system complexity and its dependency on third-parties, the possibility to operate in the absence of a reference signal is considered. Specifically, a forward scatter radar approach is exploited by extracting the target signature based on the square modulus of the surveillance signal [5]. An appropriate adaptation is presented to be able to operate with transmissions of opportunity of a pulsed type.
The second assumption made in [1] was founded on the availability of ancillary information provided by external systems. This could be a reasonable assumption if the conceived sensor operates in conjunction with other surveillance systems. However, this represents a severe limitation if the WiFi-based PFSR has to be operated stand-alone. Therefore, in this paper we investigate autonomous approaches to target motion estimation based on a time-frequency analysis and on the exploitation of a couple of Rx antennas displaced along the cross-baseline direction.
The resulting WiFi-based PFSR scheme is tested against experimental datasets collected by means of a dedicated acquisition campaign. In particular, the automatic vehicles classification capability is analysed and compared to that obtained with the processing scheme employed in [1]. The reported results show that the stand-alone sensor allows comparable classification performance with respect to the approach in [1] with the interesting advantages of reduced system complexity and autonomous operation.
The paper is organized as follow. Section 2 illustrates the Wi-Fi-based PFSR concept and the employed dataset. The conceived strategies to guarantee the stand-alone operation are addressed in Section 3. Section 4 reports the experimental results obtained at the classification stage when employing the autonomously extracted target signatures. Finally, our conclusions are drawn in Section 5.

2 WiFi-based Passive FSR sensor

The considered FSR geometry and the processing scheme for vehicle classification adopted in [1] are depicted in the left-hand side of Figure 1. Specifically, the main processing steps required to achieve the automatic target classification are reported in a shadowed box.

A commercial WiFi access point (AP) is used as transmitter of opportunity (Tx) while a receiver Rx (known as surveillance channel) is adopted to collect returns from the observed scene. The considered target moves with velocity V on a trajectory orthogonal to the Tx-Rx baseline. The vehicle signature is extracted by means of the following steps [1],[6]:

1) cross-correlation between the reference (s_{ref}) and the surveillance (s_{surv}) signals on a pulse-by-pulse basis, evaluated at delay bin equal to direct signal propagation delay;
2) collection of the samples obtained across consecutive transmitted pulses to form the target time-domain profile;
3) target profile resampling and scaling into a common axis, i.e. the spatial displacement along the cross-baseline direction, based on a proper estimate of the target velocity component along that direction;
4) application of an appropriate classification approach against the obtained signatures.

Notice that step 1) requires the availability of the reference signal, namely a good copy of the signal emitted by the AP. In the considered scenarios, as the employed sensor is installed very close to the WiFi AP exploited as illuminator of opportunity, the Tx can be assumed partially cooperative and the reference signal can be spilled directly from the Tx antenna using a directional coupler (see Figure 1). Nevertheless, the collection of this signal requires a dedicated Rx channel.

Similarly, step 3) at least requires the knowledge of the target motion component along the cross-baseline direction. In [1] we assumed that this was provided by an external cooperative system and this makes the conceived sensor dependent on the availability of ancillary information.

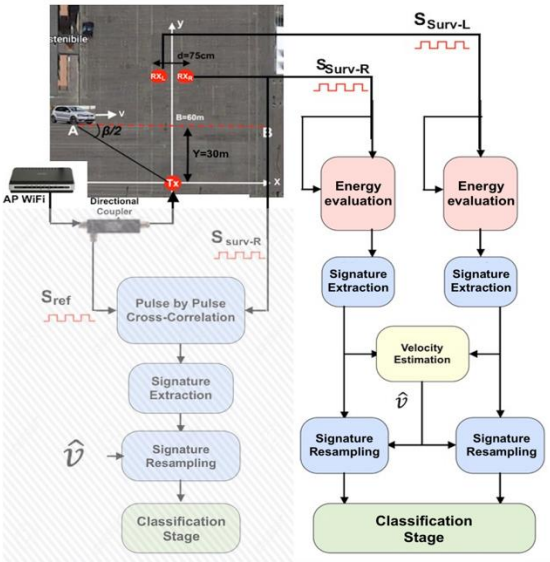

Figure 1. WiFi-based PFSR processing scheme for vehicle classification.

In this paper we overcame the above limitations by adopting alternative approaches at the signatures extraction stage. The proposed processing scheme will be then tested against the same experimental dataset used in [1] in order to provide a fair comparison among different approaches.

The considered dataset has been collected by means of the WiFi-based PR receiver developed at Sapienza University of Rome [7]. Different cars were employed as cooperative targets in the acquisition geometry sketched on the upper left corner of Figure 1. All the employed antennas were mounted at about 1.25 m of height with respect to the ground. The Tx antenna is located in (x_{Tx},y_{Tx})=(0,0) and two Rx antennas (Rx_L and Rx_R) were employed in forward scatter configuration with respect to the Tx with baseline B=60 m. This allows to perform simultaneous collection of the forward scatter target signatures perceived under two slightly different geometries and to test the robustness of the system against small antenna displacement. In fact, the Rx antennas were displaced in the horizontal direction by d=75 cm and located in (x_{Rx_L},y_{Rx_L})=(-d/2,B) and (x_{Rx_R},y_{Rx_R})= (d/2,B). The cars were moving orthogonally to the Tx-Rx baseline, from point A≈(-35 m, B/2) to point B≈(35 m, B/2) with velocity of about 4-6 m/s depending on the considered test.

3 Modifications to the signature extraction stage

The proposed modification to the signature extraction stage of the conceived WiFi-based PFSR sensor are depicted in the right-hand side of Figure 1 and illustrated in more detail in the following sub-sections.

3.a Reference signal-free system

Aiming at reducing the system complexity and its dependency on third-parties, the possibility to operate in the absence of a reference signal is considered. To this purpose, a forward scatter radar approach is exploited by extracting the target signature based on the square modulus of the surveillance signal. Specifically, the block performing the cross-correlation between the reference and surveillance signals is replaced by a processing block that simply evaluates the energy of the surveillance signal on a pulse-by-pulse basis:

$$E_m = \int \left| s_{surv_m}(t) \right|^2 \cdot dt \qquad (1)$$

Therefore, the target signature observed along the acquisition time can be formed as:

$$\underline{E} = [E_0\ E_1\ \ldots\ E_{M-1}] \qquad (2)$$

where M is the number of pulses included in the profile.

Notice that the output of (1) can be interpreted as an approximation of the zero-lag cross-correlation between the reference and the surveillance signal obtained by exploiting the received signal as a reference. Therefore, it is expected that this approach provides comparable results with respect to the conventional cross-correlation when the direct signal is the dominant contribution in the received signals. As an example, Figure 2 shows the comparison of the target signatures obtained with conventional cross-correlation between the

reference and the surveillance signal and with the proposed reference signal free approach. The results are reported for the Rx_R, when a VW Polo is employed as cooperative target. As it is apparent, the two obtained profiles are quite comparable and only slightly differences are observed when the target crosses the baseline since it partially blocks the direct signal impinging on the Rx antenna.

As an alternative to the interpretation above, the result in (1) can be regarded as a low-pass filtered version of the surveillance signal square modulus, with a filter bandwidth set by the inverse of the single pulse duration. Therefore, if the target FSR signature is slowly varying within single pulses, the proposed solution is equivalent to the approach commonly employed in active FSR systems exploiting a continuous wave transmission.

3.b Autonomous estimation of cross-baseline target velocity

In order to obtain a stand-alone capability of estimating the target velocity along its trajectory, we exploit the availability of a couple of Rx antennas displaced along the cross-baseline direction.

Specifically, based on the considered geometry, we observe that the crossing target yields similar profiles at the two Rx channels with a temporal displacement Δt depending on the target cross-baseline velocity V and the crossing point within the baseline; we indicate the latter using the distance Y of the target from the Tx antennas at the crossing point. Specifically, we can write:

$$\Delta t = \frac{d \cdot Y}{B} \cdot \frac{1}{V} \tag{3}$$

As an example, Figure 3(a) reports the signatures simultaneously extracted by the two available antennas during the same test considered in Figure 2. Their temporal displacement can be estimated by evaluating the cross-correlation between the two obtained profiles and selecting the delay yielding the maximum output as depicted in Figure 3(b). The obtained delay can be then used to provide an estimate of the target velocity assuming the prior knowledge of the crossing point Y. In the experiment reported in Figure 3, we obtain Δt=0.0796 s and, by setting $Y=B/2$, the estimated velocity is 4.71 m/s which is well in line with the value 4.74 m/s provided by the external cooperative sensor.

Notice that the approach above could be reasonably adopted when monitoring the vehicular traffic along a street where cars must remain inside the roadway, hence the crossing point can be assumed a priori known.

In other surveillance scenarios, the estimation of the crossing point is also required in order to solve the equation in (3). Therefore, another relation among the relevant parameters should be used to build up and solve a system of equations with two unknowns (i.e. V and Y).

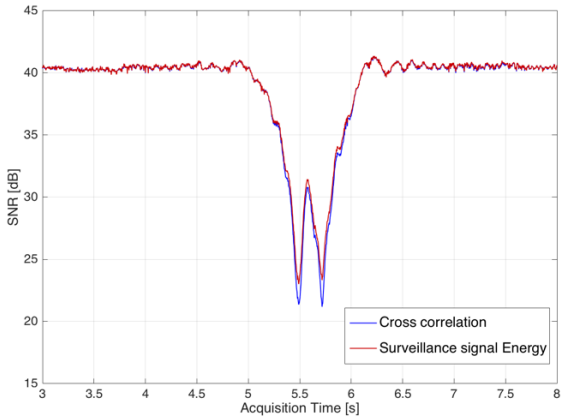

Figure 2. Comparison of the signatures obtained for a VW Polo with a conventional cross-correlation approach or by evaluating the surveillance signal energy.

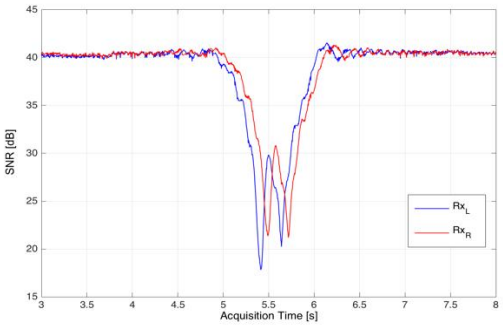

(a)

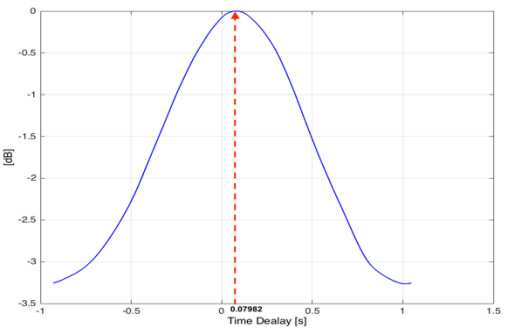

(b)

Figure 3. Results for the test with a VW Polo: (a) signatures extracted from the two Rx channels; (b) cross-correlation based time delay estimation.

In order to jointly estimate both parameters V and Y, we simultaneously exploit the estimate of the temporal displacement Δt in (3) and the estimate of the target response Doppler rate of change α that is mapped into the received profile amplitude variation thanks to the FSR principle [2]. This parameter jointly depends on the crossing point Y and on the target velocity orthogonal to the baseline as follows:

$$\alpha = \frac{1}{\lambda} \frac{V^2}{Y(B-Y)} \tag{4}$$

It can be estimated based on different methods.

A first solution is provided by the time-frequency analysis of the obtained profiles based on the evaluation of the corresponding spectrogram. An example along this line is

reported in Figure 4 where the spectrogram of one of the signatures in Figure 2 is shown. As expected, after the removal of the DC component based on a moving average scheme, a typical 'V' shape is observed as the target approaches, crosses, and then moves away from the baseline. By estimating the slope of such shape around the crossing point, we could get a reasonable estimate of the Doppler rate of change α. The sought parameter can be extracted, for example, by Radon transforming the spectrogram and then selecting the line integral yielding the highest value [11]. As an example, using this approach in the test reported in Figure 4, we obtain Y=29.58 m and V=4.81 m/s.

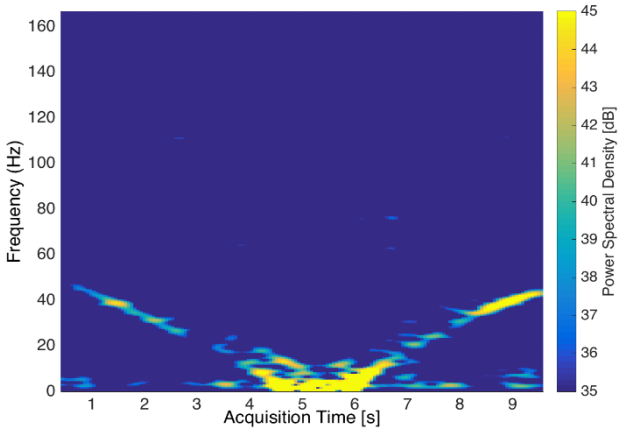

Figure 4. Spectrogram of the signature obtained for a VW Polo.

An alternative method to estimate the Doppler rate of change α is based on the direct estimate of the target chirp signature by exploiting a single longer processing interval about the crossing point and applying a procedure similar to that adopted in [10]. To this purpose, we remove the DC component affecting the received signature and we model the residual target contribution as a sine with argument varying according to a second order polynomial law. In such conditions, a dechirping approach can be exploited by looking for the positive value of the second order coefficient than yields the best focused output according to a proper criterion (e.g., an entropy minimization criterion can be adopted at this stage).
In Figure 5 we report the entropy cost function obtained for the test in Figure 2 as a function of the Doppler rate of change α. By using this approach we obtain V=4.77 m/s and Y=30.3 m.
Based on the analysis performed on the whole dataset, this second method appears to be more robust than that based on the evaluation of the spectrogram. Therefore, in the following, we adopt this second approach (together with the estimate of the relative delay in (3)) when the joint estimation of V and Y is sought.
We couldn't perform a detailed analysis of the achievable estimation accuracy of the proposed methods since the available ground-truth was in turn based on an external cooperative sensor whose accuracy cannot be easily measured. However, since the estimated parameters are just used for target's signature resampling, the impact of the proposed approaches is evaluated in Section 4 on the final classification stage exploiting the resampled profiles.

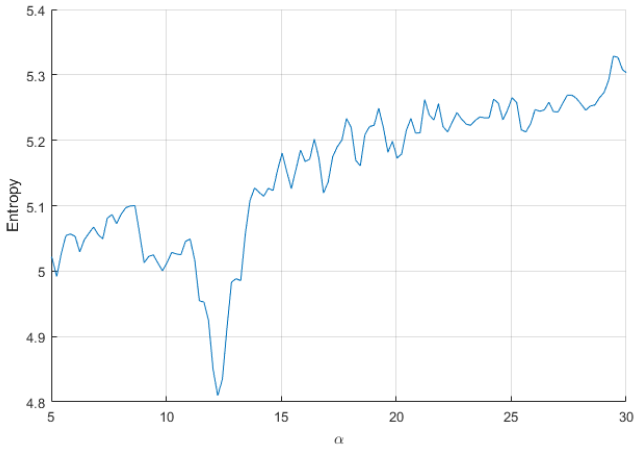

Figure 5: Entropy cost function obtained for the test employing VW Polo.

4 Automatic vehicles classification

Aiming at understanding the classification capability achieved by the WiFi-based PFSR sensor after the proposed modifications to the signature extraction stage, we exploit the classification approach and the experimental dataset illustrated in [1]. Specifically, we considered the cascade of a Principal Component Analysis (PCA)-based sub-space selection and a k-Nearest Neighbour (k-NN) algorithm as a practical and effective solution. The car models employed in the experimental tests are summarized in Table 1 where also the number of tests repeated with each vehicle is reported. Overall, based on the two Rx channels, 196 signatures where extracted and subdivided into a training set (51 profiles) and a validation set 145 profiles). Further details are reported in [1].

Table 1. Car models employed in the acquisition campaign.

Car model	Dimensions (l, w, h)	N. of tests	Label
VW Polo	3.97 x 1.65 x 1.45 m	19	1
Ford Fiesta	3.93 x 1.76 x 1.49 m	19	2
Nissan Micra	3.71 x 1.54 x 1.54 m	21	3
Fiat Punto	4.04 x 1.69 x 1.49 m	20	4
Opel Corsa	3.81 x 1.64 x 1.44 m	19	5

The classification results obtained against the target signatures extracted with the approach in [1] are firstly reported in Table 2 as a benchmark for the proposed modifications. Specifically, Table 2 reports the confusion matrix obtained at the output of the classification stage by evaluating, on a car model basis (see Table 1), the number of tests classified into each of the 5 available classes. As is apparent, only few misclassified tests are observed.
Table 3 reports the classification results obtained against the vehicles signatures resulting from the reference signal-free procedure described in Section 3.
As is apparent, identical results are achieved as those reported in Table 2; this clearly shows that removing the assumption of

perfect knowledge of the transmitted signal does not affect the proposed system performance as meaningful target signatures can be built using the surveillance signal only.

In Table 4 we show the results obtained when the target velocity is estimated using the approach proposed in section 3.b when the baseline crossing point is assumed known. It is worth noticing that only a few additional errors appear when avoiding the exploitation of the reference signal and using the estimated target velocity.

When the baseline crossing point and the target velocity are jointly estimated using the complete stand-alone method introduced in section 3.b, the results in Table 5 are obtained. Again, a remarkable classification capability is obtained (higher than 92%) against the available dataset despite the employed vehicles belong to the same cars category and possibly show a similar shape.

Table 2. Classification performance obtained with the approach considered in [1].

		Actual Labels					
Total=145		1	2	3	4	5	
Predicted Labels	1	28	0	0	0	0	28
	2	0	26	0	0	1	27
	3	0	0	31	0	0	31
	4	0	0	0	30	0	30
	5	0	2	0	0	27	29
		28	28	31	30	28	

Table 3. Classification performance obtained with the reference signal-free approach.

		Actual Labels					
Total=145		1	2	3	4	5	
Predicted Labels	1	28	0	0	0	0	28
	2	0	26	0	0	1	27
	3	0	0	31	0	0	31
	4	0	0	0	30	0	30
	5	0	2	0	0	27	29
		28	28	31	30	28	

Table 4. Classification performance obtained with the reference signal-free approach when the target velocity is estimated and the baseline crossing point is assumed known.

		Actual Labels					
Total=145		1	2	3	4	5	
Predicted Labels	1	27	0	0	0	4	31
	2	0	26	0	0	1	28
	3	0	0	31	0	0	31
	4	1	0	0	30	0	31
	5	0	2	0	0	23	25
		28	28	31	30	28	

Table 5. Classification performance obtained with the reference signal-free approach when target velocity and the baseline crossing point are jointly estimated as described in section 3.b.

		Actual Labels					
Total=145		1	2	3	4	5	
Predicted Labels	1	28	0	0	1	2	31
	2	0	22	0	0	1	23
	3	0	0	31	1	0	32
	4	0	0	0	28	0	28
	5	0	6	0	0	25	31
		28	28	31	30	28	

6 Conclusions

In this paper proper strategies have been introduced to guarantee the stand-alone operation for a WiFi-based Passive Forward Scatter Radar to be employed for vehicles automatic classification. Specifically, aiming at reducing the system complexity and its dependency on third-parties, we considered the possibility to operate in the absence of a reference signal and without any ancillary information on the target motion. This allowed to extend the results reported in the companion paper [1] where simplifying assumptions were made about the availability of the information above.
The resulting WiFi-based PFSR scheme has been tested against experimental datasets showing that the conceived stand-alone sensor provides a remarkable automatic vehicles classification capability, which is only slightly degraded with respect to that obtained in [1].
Future works will include new test campaigns aiming to investigate the impact of the observation geometry on the achievable classification results (e.g. target trajectories not necessarily orthogonal to the baseline, different crossing points, etc.) along the line suggested in [9].

References

[1] A. Losito, M. Stentella, T. Martelli, F. Colone, “Automatic vehicles classification approaches for WiFi-based Passive Forward Scatter Radar”, submitted to the Int. Conf. on Radar Systems RADAR 2017.

[2] M. Cherniakov (Ed.), Bistatic Radar: principles and practice, John Wiley & Sons, UK, 2007.

[3] M. Cherniakov et alii, "Automatic ground target classification using forward scattering radar," in IEE Proc. Radar, Sonar & Navigation, vol. 153, no. 5, pp. 427-437, Oct. 2006.

[4] F. Colone, P. Falcone, C. Bongioanni and P. Lombardo, "WiFi-Based Passive Bistatic Radar: Data Processing Schemes and Experimental Results," in IEEE Trans. on Aerospace and Electronic Systems, vol. 48, no. 2, pp. 1061-1079, April 2012.

[5] M. Gashinova, L. Daniel, V. Sizov, E. Hoare and M. Cherniakov, "Phenomenology of Doppler forward scatter radar for surface targets observation", IET Radar Sonar & Navigation, vol. 7, no. 4, pp. 422-432, April 2013.

[6] T. Martelli, F. Colone, P. Lombardo, “First Experimental Results for a WiFi-Based Passive Forward Scatter Radar”, in IEEE Radar Conference 2016.

[7] Macera, A., Bongioanni, C., Colone, F., Lombardo, P., "Receiver architecture for multi-standard based Passive Bistatic Radar," IEEE Radar Conference 2013.

[8] M. Cherniakov, R.S.A Raja Abdullah, P. Jančovič and M. Salous, “Forward Scattering Micro Sensor for Vehicle Classification”, in IEEE Int. Radar Conference 2005.

[9] A. De Luca, M. Contu, S. Hristov, L. Daniel, M. Gashinova, M. Cherniakov, “FSR Velocity Estimation Using Spectrogram”, in Radar Symposium (IRS), 2016 17th International.

[10] Colone F. et al., "WiFi-based passive ISAR for high-resolution cross-range profiling of moving targets." IEEE Transactions on Geoscience and Remote Sensing 52.6 (2014): 3486-3501.

[11] Hoilund, Carsten. "The radon transform." *Aalborg University* 12 (2007).